A Second-Order Adaptive Agent Network Model for Social Dynamics in a Classroom Setting

Nicholas, Kasper; Zonneveld, Eric; Treur, Jan

published in
Intelligent Computing Methodologies
2020

DOI (link to publisher)
10.1007/978-3-030-60796-8_14

document version
Publisher's PDF, also known as Version of record

A Second-Order Adaptive Agent Network Model for Social Dynamics in a Classroom Setting

Kasper Nicholas, Eric Zonneveld, and Jan Treur(✉)

Social AI Group, Vrije Universiteit Amsterdam, Amsterdam, The Netherlands
kasperanicholas@gmail.com, eric.zonneveld0@gmail.com, j.treur@vu.nl

Abstract. Alcohol consumption among young adolescents is problematic as health implications and behavioural changes are common consequences. Another problematic factor among young adolescents is the amount of delinquencies committed. In this paper an adaptive social agent network model using friendship relationships as predictor for alcohol consumption and amount of delinquencies committed is explored. The proposed agent network model was empirically validated using classroom data on young adolescents gathered by Knecht in Dutch schools. The agent network model is second-order adaptive and applies a bonding by homophily adaptation principle with adaptive adaptation speed describing clustering in friends networks based on the two aforementioned factors respectively.

Keywords: Social dynamics · Agent network model · Second-order adaptive

1 Introduction

Drinking alcohol on a daily basis is a widely accepted practice and is often seemingly inseparable from social interactions in many modern day societies. However, health consequences due to alcohol consumption are a common occurrence, and can be especially problematic at a young age [1, 5–7, 10, 12, 14, 15, 19]. Both online and offline interaction among young people have been shown to contribute to increased alcohol consumption [10, 12]. As alcohol is often considered a social cohesive, it is logical to study the relation between social networks and alcohol consumption in order to assess any potential causality. Especially during early adolescence do social interactions among peers become increasingly important influential factors. A phenomenon closely related to this is bonding-by-homophily, which expresses the increased occurrence of interactions between similar persons compared to dissimilar persons [2, 13, 16]. An extensive study done by Knecht et al. [10] in 2010 aims to shed light on the effects of this bonding principle and potential social influences among adolescent friends in Dutch schools. They observed that, despite the varying friendship dynamics and individual drinking behaviour, the social network dynamics are a recurring element for the prediction of alcohol consumption among young adolescents. In a similar way they analysed the relation to delinquencies committed by young adolescents.

D.-S. Huang and P. Premaratne (Eds.): ICIC 2020, LNAI 12465, pp. 161–173, 2020.
https://doi.org/10.1007/978-3-030-60796-8_14

The conceptual idea of social agent networks is a useful basis to formalise and analyse the above processes computationally. Computational formalisation can be a good basis for the development of tools to explore the complex and phenomena as described above and support societal decision making. One of the proposed computational methods to study such social dynamics in agent networks is the Network-Oriented Modelling approach presented in [18]. This generic AI modelling approach is based on (adaptive) causal relations incorporating a continuous time dimension to model agent network dynamics and adaptivity; it is briefly introduced in Sect. 2. A number of studies have shown that this computational modeling method can be used to model a variety of social networks; e.g., [3, 4, 8, 11, 18]. Together with the scientific domain literature indicated above, this modeling perspective provides an adequate multidisciplinary research background for the work reported here.

As a main contribution, in this paper a second-order adaptive social agent network model addressing the above processes is described (in Sect. 3) and explored by simulation experiements (in Sect. 4). The social agent network model incorporates the social contagion principle, the first-order adaptive bonding by homophily principle, and a second-order principle for adaptive speed of first-order adaptation. The agent network model was verified by means of mathematical analysis of equilibria (see Sect. 5). Validation was done by the analysis of a data set on alcohol consumption and delinquencies among Dutch high school students [10]; this is discussed in Sect. 6. In order to assess the formation of friendships based on both factors, subsequent parameter tuning was performed by means of Simulated Annealing [9]. The second-order adaptivity and the validation using these empirical data distinguish this work from existing work. Finally, Sect. 7 is a discussion.

2 The Adaptive Modelling Approach for Agent Networks

Network-Oriented Modelling [18] based on temporal-causal networks uses nodes and connections between these nodes as a basic representation. The former are interpreted as states, or states variables, whereas the latter model causal relationships between such states, and have weights as labels. Both states and (in adaptive networks) connections are allowed to vary over time, and thus give rise to dynamics within the network and adaptivity of the network. The design of a network model on a conceptual level is specified as a labeled graph or in a conceptual role matrix specification format [18]. Table 1 summarizes the main concepts. Firstly, *states* and *connections* between them representing causal impacts of the states upon each other. Secondly, the notion of a *connection weight* expresses the strength of impact of a connection. *Combination functions* are used to aggregate the combined influence of states on a given state, and *speed factors* represent the rate of change of a given state with respect to time.

Table 1. An overview of the important concepts in conceptual temporal-causal networks.

Concepts	Notation	Explanation
States and connections	X, Y, $X \rightarrow Y$	Denotes the nodes and edges in the conceptual representation of a network
Connection weights	$\boldsymbol{\omega}_{X,Y}$	A connection between states X and Y has a corresponding *connection weight*. In most cases: $\boldsymbol{\omega}_{X,Y} \in [-1, 1]$
Aggregating multiple impacts on a state Y	$\mathbf{c}_Y(..)$	Each state has a *combination function* which is responsible for combining causal impacts of all states from which Y gets incoming connections
Timing of the effect of causal impact	$\boldsymbol{\eta}_Y$	The *speed factor* determines how fast a state changes by any aggregated causal impact. In most cases $\boldsymbol{\eta}_Y \in [0, 1]$

A large variety of combination functions can be used for different states in temporal-causal networks, providing sufficient flexibility for the aggregation of causal impact of states upon one another. The choice of a combination function largely depends on the application at hand, and can further be varied between states in the same system. Combination functions that are often used are briefly elaborated upon in Table 3. The numerical representations based on the above defined conceptual framework is presented in Table 2.

Table 2. Overview of the numerical representations for temporal-causal network models.

Concept	Representation	Explanation
State values over time t	$Y(t)$	At each time point t any state Y has a real number value, usually in [0, 1]
Single causal impact	$\mathbf{impact}_{X,Y}(t) = \boldsymbol{\omega}_{X,Y} X(t)$	For every time point t state X with connection to state Y impacts Y, through connection weight $\boldsymbol{\omega}_{X,Y}$
Aggregating multiple impacts	$\mathbf{aggimpact}_Y(t)$ $= \mathbf{c}_Y(\mathbf{impact}_{X_1,Y}(t), \ldots, \mathbf{impact}_{X_k,Y}(t))$ $= \mathbf{c}_Y(\boldsymbol{\omega}_{X_1,Y}X_1(t), \ldots, \boldsymbol{\omega}_{X_k,Y}X_k(t))$	The aggregated causal impact of multiple states X_i on Y at t, is determined using a combination function $\mathbf{c}_Y(V_1, \ldots, V_k)$ applied to the single causal impacts
Timing of the causal effect	$Y(t+\Delta t) = Y(t)$ $+ \boldsymbol{\eta}_Y[\mathbf{aggimpact}_Y(t) - Y(t)]\,\Delta t$ $= Y(t) + \boldsymbol{\eta}_Y[\mathbf{c}_Y(\boldsymbol{\omega}_{X_1,Y}X_1(t),$ $\ldots, \boldsymbol{\omega}_{X_k,Y}X_k(t)) - Y(t)]\,\Delta t$	The speed factor $\boldsymbol{\eta}_Y$; determines how fast a state changes upon aggregated impact of the states X_i from which state Y has incoming connections

The obtained *difference equation* or its equivalent *differential equation* in the last row of Table 2 is important for both simulation and mathematical analysis of a network model. When a (first-order) *adaptive* temporal-causal network model is considered,

network characteristics such as the connection weights, speed factors and combination functions can explicitly be represented themselves as network states, called reification states [18], and thus also evolve over time according to a difference equation of the type presented above for them. Such (first-order) reification states can be depicted as a separate level in the network picture, called first-order reification level. As this process of network reification can be repeated to obtain higher-order adaptation, in this way multiple levels can be distinguished, as illustrated for second-order adaptation by the example network model in Fig. 1.

Several examples of combination functions in adaptive temporal-causal networks are used in literature such as [3, 8, 11]; see Table 3 for some of them. The first is the *identity* **id(.)** for a single state impacting another state. The second is the *scaled sum* **ssum(..)** with a scaling factor λ. The third is the *advanced logistic sum* $\mathbf{alogistic}_{\sigma,\tau}(..)$ with parameters **σ** for the steepness and **τ** for the threshold. These and other combination functions are further explained in [18], Chap. 2. A fourth combination function discussed is the *simple linear homophily function* **slhomo,(..)**, where is a homophily modulation factor and is a homophily tipping point. For an in depth derivation of this function Sect. 3. In Table 3 a mathematical representation of each of the four combinations functions is presented. In the $\mathbf{slhomo}_{\alpha,\tau}(V_1, V_2, W)$ combination function, the variable W stands for the value of the connection weight reification state used in the adaptive network.

Table 3. An overview of some combination functions. The latter two are used in the adaptive social agent network model presented here.

Combination function	Description	Formula $c_Y(..)$ =
$\mathbf{id}(V)$	Identity	V
$\mathbf{ssum}_{\lambda}(V_1, ..., V_k)$	Scaled sum	$\frac{V_1 + ... + V_k}{\lambda}$ with $\lambda > 0$
$\mathbf{alogistic}_{\sigma,\tau}(V_1, ..., V_k)$	Advanced logistic sum	$\left[\frac{1}{1+e^{-\sigma(V_1+...+V_k-\tau)}} - \frac{1}{1+e^{\sigma\tau}}\right](1+e^{-\sigma\tau})$
$\mathbf{slhomo}_{\alpha,\tau}(V_1, V_2, W)$	Standard linear homophily	$W + \alpha\,(\tau - \lvert V_1 - V_2\rvert)(1 - W)W$

3 The Adaptive Agent Network for Bonding by Homophily

In this section the second-order adaptive social agent network model for bonding by homophily is introduced. In [18] it is shown how the design of adaptive agent network models can be addressed in a principled manner. First, note that at the base level (non-adaptive) dynamics of the states in the form of social contagion is modeled. By this, the state values mutually affect each other through the connections with their weights. In this way there is a causal pathway from connection weights to state values. Next, a first form of adaptivity (first-order adaptation) addresses the dynamics of the connection weights between two persons A and B. In particular, bonding by homophily describes

how these connections are affected by the activation levels of the states *A* and *B*. To make this more precise, the effect of the state activation levels on the connection weights must be determined. This is where the homophily principle is detailed further:

- Activation values close to one another exert an upward pressure on connection weight $\omega_{A,B}$; activation levels for *A* and *B* distant from each other exert downward pressure on $\omega_{A,B}$

In this way, a causal pathway occurs from state values to connection weights. Therefore there is a circular causal relation between state values and connection weights. In other words, it becomes hard to distinguish between the causes and the consequences, as is discussed more in depth in [2, 15–17].

To incorporate the described effect of bonding by homophily on the connection weights in a numerical manner, for any agents *A* and *B* in the base level network, representations in terms of first-order network reification states $\mathbf{W}_{B,A}$ and their network characteristics are required. The change in $\mathbf{W}_{B,A}$ will depend on a yet to be chosen combination function $\mathbf{c}_{\mathbf{W}_{B,A}}(V_1, V_2, W)$; the general difference equation becomes

$$\mathbf{W}_{B,A}(t+\Delta t) = \mathbf{W}_{B,A}(t) + \boldsymbol{\eta}_{\mathbf{W}_{B,A}}\left[\mathbf{c}_{\mathbf{W}_{B,A}}(\mathrm{A}(t), \mathrm{B}(t), \mathbf{W}_{B,A}(t)) - \mathbf{W}_{B,A}(t)\right]\Delta t$$

and the *differential equation* becomes:

$$\mathrm{d}\mathbf{W}_{B,A}(t)/\mathrm{dt} = \boldsymbol{\eta}_{\mathbf{W}_{B,A}}\left[\mathbf{c}_{\mathbf{W}_{B,A}}(\mathrm{A}(t), \mathrm{B}(t), \mathbf{W}_{B,A}(t)) - \mathbf{W}_{B,A}(t)\right]$$

As shown in [18], Chap. 13, a simple linear homophily combination function with connection weight reification state $\mathbf{W}_{B,A}$ for the connection from agent *A* to agent *B* can be obtained by the following combination function (also shown in Table 3):

$$\mathbf{c}_{\mathbf{W}}(V_1, V_2, W) = \mathbf{slhomo}_{\boldsymbol{\alpha},\boldsymbol{\tau}}(V_1, V_2, W) = W + \boldsymbol{\alpha}(\boldsymbol{\tau} - |V_1 - V_2|)(1 - W)W$$

The parameters $\boldsymbol{\alpha}$ and $\boldsymbol{\tau}$ can be chosen as required for the model at hand. The term $W(1 - W)$ ensures adequate bounding within [0, 1].

On top of the first-order adaptive social agent network model described above, a second-order adaptation level is built. This is used to make the adaptation speed of the first-order adaptation, adaptive itself. For this, second-order reification states $\mathbf{H}_{\mathbf{W}_{B,A}}$ are introduced, indicating in a dynamic manner the speed of change for the connection weight $\mathbf{W}_{B,A}$ from agent *B* for agent *A*. For the states $\mathbf{H}_{\mathbf{W}_{B,A}}$ the combination function $\mathbf{alogistic}_{\boldsymbol{\sigma},\boldsymbol{\tau}}(V_1, \ldots, V_k)$ was used.

So, within the adaptive social agent network model, each of the agents is modeled by a *three-level agent model* for a second-order adaptive social agent, consisting of a number of states and their connections:

- *base state Y* for the agent
- *first-order reification states* $\mathbf{W}_{X_1,Y}, \ldots, \mathbf{W}_{X_k,Y}$ for the weights of all of *Y*'s adaptive incoming connections
- *second-order reification states* $\mathbf{H}_{\mathbf{W}_{X_1,Y}}, \ldots, \mathbf{H}_{\mathbf{W}_{X_k,Y}}$ for the adaptive learning rates of each of the incoming connections for *Y*

For a more detailed overview of the connectivity within this adaptive agent model, see Table 4; for a simple example for only one first-order reification state and one second-order reification state, see the pink oval in Fig. 1.

Table 4. Overview of the different types of states, their roles, and their connectivity (as used in the simulations)

State		Role	Connectivity in the network
Name	Number		
A,.., I	X_1, …, X_9	Base states for the different agents	• All mutually connected (72 black arrows in the base plane) • For each Y of them 8 incoming connections from the first-order reification states $\mathbf{W}_{X_i,Y}$ (8 blue downward arrows) • For each Y of them 8 outgoing connections to $\mathbf{W}_{X_i,Y}$ and 8 outgoing connections to $\mathbf{H}_{\mathbf{W}_{X_i,Y}}$ (16 blue upward arrows)
$\mathbf{W}_{X,Y}$	X_{10}, …, X_{81}	Connection weight reification states for the base connections from X to Y	• An outgoing connection to Y to provide the adaptive weight for the connection from X to Y (red downward arrow) • An outgoing connection to $\mathbf{H}_{\mathbf{W}_{X,Y}}$ (blue upward arrow) • Three incoming connections: from X and Y (blue upward arrow) and from itself
$\mathbf{HW}_{X,Y}$	X_{82}, …, X_{153}	Speed factor reification states for states $\mathbf{W}_{X,Y}$	• An outgoing connection to $\mathbf{W}_{X,Y}$ to provide the adaptive speed factor for $\mathbf{W}_{X,Y}$ (red downward arrow) • Four incoming connections from X and Y, and from $\mathbf{W}_{X,Y}$ (blue upward arrows) and from itself

Note that the three-layered social adaptive agent model for agent Y as a whole only has incoming connections from X_1, …, X_k; internally these inputs are processed in parallel at each of the three levels. Note that the red downward arrows define special effects according to the role played by the reification state. For example, in the difference equation from Table 2, for reification state $\mathbf{W}_{B_i,A}$ (playing the role of connection weight) its value is used as connection weight $\boldsymbol{\omega}_{B_i,A}$, and for reification state $\mathbf{H}_{\mathbf{W}_{B_i,A}}$ (playing the role of speed factor) its value is used as speed factor $\boldsymbol{\eta}_{\mathbf{W}_{B_i,A}}$. This is explained in more technical detail in [18], Chaps. 9 and 10.

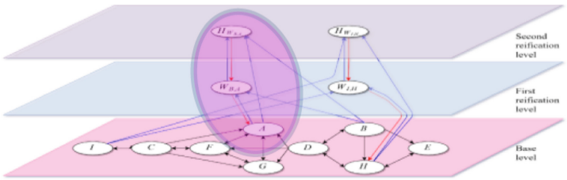

Fig. 1. A conceptual representation of the designed second-order adaptive social agent network model. Two example states are given for the first and second reification level to illustrate the effect of each state. The actual agent network model used in the simulations contains on each reification level not 2 but 9*8 = 72 reification states for the weights of all connections between the base level states and their speed factors. The pink oval depicts what together forms a three-layered model for one second-order adaptive social agent. (Color figure online)

4 Simulation Scenarios for the Agent Network Model

The designed agent network model has been compared to empirical data from one classroom from the Knecht data set [10]. To make the validation of the model more feasible, the group was split on sex and only the friendship, alcohol and delinquency data related to the male students were kept. In Table 5 all empirical data used are shown.

Table 5. The data on alcohol consumption and delinquency at four points in time with preprocessing as explained in the paper.

Alcohol	Wave 1	Wave 2	Wave 3	Wave 4	Delinquency	Wave 1	Wave 2	Wave 3	Wave 4
A	0.1	0.1	0.1	0.1	A	0.3	0.3	0.5	0.3
B	0.1	0.1	0.1	0.1	B	0.1	0.1	0.3	0.1
C	0.3	0.3	0.5	0.7	C	0.1	0.3	0.5	0.3
D	0.1	0.1	0.5	0.9	D	0.1	0.3	0.3	0.1
E	0.1	0.1	0.1	0.1	E	0.1	0.1	0.2	0.3
F	0.1	0.1	0.1	0.1	F	0.3	0.1	0.3	0.1
G	0.1	0.1	0.5	0.9	G	0.7	0.1	0.5	0.7
H	0.1	0.1	0.1	0.1	H	0.1	0.3	0.1	0.1
I	0.1	0.1	0.3	0.7	I	0.1	0.3	0.5	0.3

The initial values for the model were taken from the first wave of the remaining data. Connections in the base network mean that student *X* sees student *Y* as a friend. Since the network is directed, friendships are not always reciprocated. The network initially consists of 9 nodes and 23 edges, giving an average in-degree of 2.556. The nodes with the highest in-degree are A, F and G, which have an in-degree of 4. Two strongly connected components can be identified with B, D, E and H making up the first component and A, C, F, G, I the second component. As the friendship connections should be able to change over time each student was to some extent connected to every other student. The initial values of the connection weights that initially exist were set at 0.9, and the initial values of the other connection weights are set to the low value 0.1.

The initial values of the base states were based on the first wave alcohol or delinquency values from the Knecht dataset, depending on which of the two were simulated. The empirical data used to tune the model was based on the alcohol or delinquency data from the other waves. However, some of the data was missing for certain students at certain time points. Linear interpolation was used to create values for those entries. The values for alcohol and delinquency were normalised between 0.1 and 0.9 for the model. The initial values of the 72 (first-order) **W** states are either 0.1 or 0.9, depending on if initially a recognized friendship exists between the nodes in the network. The initial values of all 72 (second-order) **H** states were 0.1.

5 Empirical Validation of the Adaptive Agent Network Model

Running the model described in the previous section with hand-set values for the network characteristics until $t = 20$ with $\Delta t = 0.1$ for alcohol and delinquency values separately provided results as shown in Fig. 2 with a Root Mean Square Error (RMSE) between the empirical data and results of 0.7017 and 0.6866 for alcohol and delinquency respectively. Clustering was observed, but the results do not correspond to the empirical data, which is why a high RMSE occurs.

Fig. 2. The 9 state values of the network are presented for both alcohol (on the left) and delinquencies (on the right) with respect to time.

In order to reduce the RMSE, the model was tuned more systematically to get values for the network characteristics that correspond more to the real world. In the first experiment, the speed factors of the base states were tuned using Simulated Annealing with roughly 5000 iterations, while keeping all other parameters the same [9]. This give the results for alcohol and for delinquency shown in Fig. 3. The RMSE and resulting parameter values are shown in Table 6. The RMSE for these models is significantly lower than for the simple models. Note that the predicting alcohol usage has a slightly higher RMSE than the delinquency variant. Also observe that the speed factors are low for students that do not change their alcohol consumption or the amount of delinquencies they commited. Clusters are being formed in both simulation scenarios.

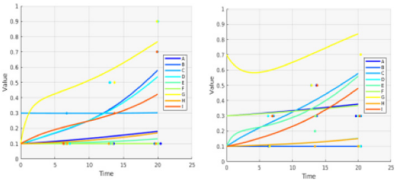

Fig. 3. The 9 state values of the network are presented for both alcohol (on the left) and delinquencies (on the right) with respect to time. The tuning of the speed values is done in both instances.

Table 6. Parameters found when tuning speed factors for alcohol and delinquency, along with the RMSE of the simulation with these parameters compared to the empirical data.

	RMSE	η_A	η_B	η_X	η_Δ	η_E	η_Φ	η_Γ	η_H	η_I
Alcohol	$1.85 * 10^{-1}$	$7.02 * 10^{-3}$	$9.90 * 10^{-1}$	$1.78 * 10^{-3}$	$2.19 * 10^{-1}$	$6.02 * 10^{-3}$	$7.42 * 10^{-5}$	$9.95 * 10^{-1}$	$9.57 * 10^{-3}$	$2.24 * 10^{-1}$
Delinquency	$1.83 * 10^{-1}$	$8.09 * 10^{-3}$	$2.49 * 10^{-3}$	$1.36 * 10^{-1}$	$1.26 * 10^{-2}$	$9.74 * 10^{-1}$	$7.02 * 10^{-3}$	$3.60 * 10^{-1}$	$6.99 * 10^{-3}$	$1.43 * 10^{-1}$

For a next experiment, again the speed factors for the base states were tuned but additionally the tipping points $\boldsymbol{\tau}$ for a few selected **W** states were tuned. These **W** states were chosen in the following manner. The nodes with the highest in-degrees were identified, being A, F and G. The students these nodes represent are thus liked by a lot of classmates. Then the outgoing edges from these nodes present in Fig. 1 were used to optimize the influence they have on the network. Again simulated annealing for roughly 5000 iterations was used to find the optimal values.

This results in the RMSE and parameters shown in Table 7 and the simulations with these parameters as shown in Fig. 4. The RMSE for both simulations is lower than in the previous experiment. The alcohol usage based model has a slightly lower RMSE than the delinquency variant. In both cases 3 clusters are formed.

Fig. 4. The 9 state values of the network are presented for both alcohol (on the left) and delinquencies (on the right) with respect to time. The tuning of both the speed values and several tipping points was done in both instances.

Table 7. Parameters found when tuning speed factors and selected tipping points for alcohol and delinquency, along with the RMSE of the simulation with these parameters compared to the empirical data.

	Alcohol	Delinquency		Alcohol	Delinquency
RMSE	$1.57 * 10^{-1}$	$1.67 * 10^{-1}$			
$\boldsymbol{\eta}_A$	$1.93 * 10^{-2}$	$9.61 * 10^{-3}$	$\tau_{W_{A,F}}$	$3.08 * 10^{-1}$	$2.53 * *10^{-1}$
$\boldsymbol{\eta}_B$	$6.41 * 10^{-1}$	$2.54 * 10^{-5}$	$\tau_{W_{A,G}}$	$2.86 * 10^{-1}$	$9.78 * 10^{-1}$
$\boldsymbol{\eta}_C$	$9.70 * 10^{-1}$	$9.30 * 10^{-3}$	$\tau_{W_{F,A}}$	$9.98 * 10^{-1}$	$9.65 * 10^{-3}$
$\boldsymbol{\eta}_D$	$9.86 * 10^{-1}$	$1.84 * 10^{-2}$	$\tau_{W_{F,C}}$	$6.73 * 10^{-1}$	$3.54 * 10^{-1}$
$\boldsymbol{\eta}_E$	$2.26 * 10^{-4}$	$2.77 * 10^{-2}$	$\tau_{W_{F,G}}$	$4.09 * 10^{-2}$	$7.52 * 10^{-1}$
$\boldsymbol{\eta}_F$	$3.36 * 10^{-3}$	$3.31 * 10^{-5}$	$\tau_{W_{G,A}}$	$4.47 * 10^{-2}$	$2.73 * 10^{-2}$
$\boldsymbol{\eta}_G$	$9.15 * 10^{-2}$	$9.82 * 10^{-1}$	$\tau_{W_{G,F}}$	$3.66 * 10^{-1}$	$1.07 * 10^{-2}$
$\boldsymbol{\eta}_H$	$3.37 * 10^{-3}$	$9.31 * 10^{-3}$			
$\boldsymbol{\eta}_I$	$9.51*10^{-1}$	$9.82*10^{-1}$			

6 Mathematical Verification of the Model

To verify that the model is mathematically correct, in [18], Chap. 12 it is observed that a state has a stationary point (i.e., d*Y(t)*/d*t* = 0) if and only if

$$\boldsymbol{\eta}_Y = 0 \quad \text{or} \quad \mathbf{aggimpact}_Y(t) = Y(t)$$

The model is in equilibrium at *t* if *all* states have a stationary point at *t*. Furthermore, from [18], Chap. 3, Sect. 3.6.1 it is concluded that (assuming speed $\mathbf{H} > 0$) for the standard linear homophily function obtain the following equilibrium equation is obtained:

$$W = \mathbf{slhomo}_{\boldsymbol{\alpha},\boldsymbol{\tau}}(V_1, V_2, W) = W + \boldsymbol{\alpha}(\boldsymbol{\tau} - |V_1 - V_2|)(1 - W)W$$

which for $\boldsymbol{\alpha} > 0$ is equivalent to:

$$(\boldsymbol{\tau} - |V_1 - V_2|)(1 - W)W = 0$$

Thus, all connection weights *W* should equal to either 0 or 1, or else $|V_1 - V_2|$ must be equal to τ. Running the model for the simulation in Sect. 5 for end time 100 and $\Delta t = 1$, the correctness of the model in the emerging equilibrium was verified. First, it was analysed if the base states have reached an equilibrium state of the network model at $t = 100$.

Table 8. Equilibrium analysis for all 9 base states, two first-order reification states and two second-order reification states in the social agent network model.

Base state X_i	A	B	C	D	E	F	G	H	I
$X_i(t)$	1.0000	1.0000	1.0000	1.0000	1.0000	1.0000	1.0000	1.0000	1.0000
aggimpact$_{X_i}$	1.0000	1.0000	1.0000	1.0000	1.0000	1.0000	1.0000	1.0000	1.0000
deviation	$3 * 10^{-10}$	$6 * 10^{-10}$	$4 * 10^{-10}$	$4 * 10^{-10}$	$4 * 10^{-10}$	$3 * 10^{-10}$	$3 * 10^{-10}$	$3 * 10^{-10}$	$5 * 10^{-10}$
2nd order state X_i	$\mathbf{H}_{WA,B}$	$\mathbf{H}_{WI,H}$	1st order state X_i					$\mathbf{W}_{A,B}$	$\mathbf{W}_{I,H}$
$X_i(t)$	0.9886	0.9886	$X_i(t)$					0.9993	0.9993
aggimpact$_{X_i}$	0.9886	0.9886	**value for equilibrium equation**					1	1
deviation	$-2.3 * 10^{-7}$	$-2.1 * 10^{-7}$	**deviation**					$7.2 * 10^{-4}$	$6.7 * 10^{-4}$

As seen in Table 8 all base states have reached a stationary point, since **aggimpact**$_Y(t) = Y(t)$. Next, it was analysed if the homophily function in the model is mathematically correct by evaluating the W states or the τ parameter value of the homophily function of these states. The complete analysis of all 144 W and H states is required for a complete mathematical verification of the proposed model. Including the verification is however beyond the scope of here presented work. Instead, two W and H states were analysed to show mathematical validity of sample states. However, the similarity between the states in both reification levels respectively indicates that the calculated validity is likely to hold for all states. The chosen first-order reification states are $\mathbf{W}_{A,B}$ and $\mathbf{W}_{I,H}$. State $\mathbf{W}_{A,B}$ has a value of 0.9993 at equilibrium, giving an error from 1 of $1 - \mathbf{W}_{A,B} = 7.2289*10^{-4}$. State $\mathbf{W}_{I,H}$ has a value of 0.9993 at equilibrium, giving an error from 1 of $1 - \mathbf{W}_{I,H} = 6.7210*10^{-4}$. The results for the corresponding **H** states are shown in Table 8 lower part. These results are further in accordance with the aforementioned theory.

7 Discussion

In this paper the dynamic and adaptive relation between friendships and alcohol consumption and the committing of delinquencies were analysed computationally by means of a second-order adaptive social agent network model. Also other network models have been previously proposed as a means to simulate social networks and the homophily principle (e.g. [2, 4, 11, 18]); however, these models are only first-order adaptive whereas in the current paper a second-order adaptive agent network model was used. In [18], also a second-order adaptive agent model was presented. However, that was a single cognitive agent model and the focus was on metaplasticity as known in Cognitive Neuroscience. In contrast, the current paper addresses a multi-agent case of a social agent network model. In [18], Sect. 6 also an adaptive social network model was modeled and simulated which is second-order adaptive. However, the second-order adaptation there has focus on adaptive tipping points and not on adaptive learning speed as in the current paper.

To provide a good fit to empirical data, initially the speed factors of the base states were tuned by Simulated Annealing for both alcohol and delinquency data. Thereafter, also multiple tipping points of the simple linear homophily combination function wre tuned. These tipping points were chosen by picking the three nodes with the highest in-degree. The model that predicted alcohol usage was slightly more accurate than the delinquency variant with RMSE values of $1.6*10^{-1}$ and $1.7*10^{-1}$ respectively. The difference in RMSE was, however, relatively insignificant. This shows that both alcohol consumption and the committing of delinquencies have been adequately illustrated by the proposed model. In both cases clustering is observed, but more for alcohol consumption compared to the committing of delinquencies, as is shown in Fig. 4. This is likely due the similarity in initial values for alcohol consumption, whereas a larger spread is observed in the initial values of the data on delinquencies. A subsequent mathematical verification further indicates the mathematical validity of the model.

A number of aspects could be further improved upon in future work. The first of which is the inclusion of more parameters in the tuning process. Secondly, the inclusion of data on a complete class or multiple classes could further improve the accuracy of clustering behaviour in the model compared to the fitted data. Additionally, a multicriteria homophily can be used to combine alcohol and delinquency data in one model, alongside other demographic information that is present in de dataset. A final improvement to the model can be to focus on the inclusion of different adaptivity mechanisms. This could for instance be implemented by creating extra adaptive states for other combination function parameters.

References

1. Ali, M.M., Dwyer, D.S.: Social network effects in alcohol consumption among adolescents. Addict. Behav. **35**(4), 337–342 (2010)
2. Aral, S., Muchnik, L., Sundararajan, A.: Distinguishing influence-based contagion from homophily-driven diffusion in dynamic networks. PNAS **106**(51), 21544–21549 (2009)
3. Blankendaal, R., Parinussa, S., Treur, J.: A temporal-causal modelling approach to integrated contagion and network change in social networks. In: Proceedings of the 22nd European Conference on Artificial Intelligence, ECAI 2016, pp. 1388–1396. IOS Press (2016)
4. van den Beukel, S., Goos, S.H., Treur, J.: An adaptive temporal-causal network model for social networks based on the homophily and more-becomes-more principle. Neurocomputing **338**, 361–371 (2019)
5. Christiansen, B.A., Smith, G.T., Roehling, P.V., Goldman, M.S.: Using alcohol expectancies to predict adolescent drinking behavior after one year. J. Consult. Clin. Psychol. **57**(1), 93–99 (1989)
6. Henneberger, A.K. Mushonga, D.R., Preston, A.M.: Peer influence and adolescent substance use: a systematic review of dynamic social network research. Adolesc. Res. Rev. (2020). https://doi-org.vu-nl.idm.oclc.org/10.1007/s40894-019-00130-0
7. Huang, G.C., et al.: Peer influences: the impact of online and offline friendship networks on adolescent smoking and alcohol use. J. Adolesc. Health **54**(5), 508–514 (2014)
8. Kappert, C., Rus, R., Treur, J.: On the emergence of segregation in society: network-oriented analysis of the effect of evolving friendships. In: Nguyen, N.T., Pimenidis, E., Khan, Z., Trawiński, B. (eds.) ICCCI 2018. LNCS (LNAI), vol. 11055, pp. 178–191. Springer, Cham (2018). https://doi.org/10.1007/978-3-319-98443-8_17
9. Kirkpatrick, S., Gelatt, C.D., Vecchi, M.P.: Optimization by simulated annealing. Science **220**(4598), 671–680 (1983)
10. Knecht, A.B., Burk, W.J., Weesie, J., Steglich, C.: Friendship and alcohol use in early adolescence: a multilevel social network approach. J. Res. Adolesc. **21**(2), 475–487 (2011)
11. Kozyreva, O., Pechina, A., Treur, J.: Network-oriented modeling of multi-criteria homophily and opinion dynamics in social media. In: Staab, S., Koltsova, O., Ignatov, D.I. (eds.) SocInfo 2018. LNCS, vol. 11185, pp. 322–335. Springer, Cham (2018). https://doi.org/10.1007/978-3-030-01129-1_20
12. McCreanor, T., Lyons, A., Griffin, C., Goodwin, I., Barnes, H.M., Hutton, F.: Youth drinking cultures, social networking and alcohol marketing: Implications for public health. Crit. Public Health **23**(1), 110–120 (2013)
13. McPherson, M., Smith-Lovin, V., Cook, J.M.: Birds of a feather: homophily in social networks. Ann. Rev. Sociol. **27**(1), 415–444 (2001)

14. Montgomery, S.C., Donnelly, M., Bhatnagar, P., Carlin, A., Kee, F., Hunter, R.F.: Peer social network processes and adolescent health behaviors: a systematic review. Prev. Med. **130**, 105900 (2020)
15. Mundt, M.P., Mercken, L., Zakletskaia, L.: Peer selection and influence effects on adolescent alcohol use: a stochastic actor-based model. BMC Pediatr. **12**(1), 115 (2012)
16. Shalizi, C.R., Thomas, A.C.: Homophily and contagion are generically confounded in observational social network studies. Sociol. Methods Res. **40**(2), 211–239 (2011)
17. Steglich, Ch., Snijders, T.A.B., Pearson, M.: Dynamic networks and behavior: separating selection from influence. Sociol. Methodol. **40**(1), 329–393 (2010)
18. Treur, J.: Network-Oriented Modeling for Adaptive Networks: Designing Higher-Order Adaptive Biological, Mental and Social Network Models. Springer, Cham (2020)
19. Zhang, J., Centola, D.: Social networks and health: new developments in diffusion, online and offline. Ann. Rev. Sociol. **45**(1), 91–109 (2019)